Stability of charged Si-doped heterofullerenes: A first-principles molecular dynamics study

Masahiko Matsubara[1] and Carlo Massobrio[2]
[1]*Laboratoire des Colloïdes, Verres et Nanomatériaux, UMR 5587 CNRS, Université Montpellier II, F-34095 Montpellier Cedex 5, France*
[2]*Institut de Physique et de Chimie des Matériaux de Strasbourg, 23 rue du Loess, BP43, F-67034 Strasbourg Cedex 2, France*
(Received 22 July 2008; revised manuscript received 12 March 2009; published 6 April 2009)

We study the structural stability of the singly and doubly charged (positively and negatively) Si-doped heterofullerene $C_{30}Si_{30}$ via density-functional theory calculations combined with first-principles molecular dynamics. Geometry optimization aimed at establishing the most stable configurations at $T=0$ K shows that $C_{30}Si_{30}$ undergoes very limited changes in the bond lengths after addition or extraction of one or two electrons. Consideration of thermal motion reveals that the dynamical stability is not significantly altered in $C_{30}Si_{30}^{-}$ with respect to the neutral case. On the contrary, Si-Si and C-C bond stretching followed by rapid fragmentation, occurring in less than 1 ps, are observed for $C_{30}Si_{30}^{--}$. This effect is encountered in two sets of calculations performed with the periodic cell and the isolated cell boundary conditions for the heterofullerene. In the periodic case, fragmentation is due to the predominance of Si atoms carrying charges of equal sign in the Si-rich portion of the cage. In the isolated case, the number of neighboring charges of equal sign is reduced but the strength of the residual repulsive interaction is sufficient to destabilize the network at finite temperature. The lack of stability of doubly charged Si-doped heterofullerenes confirms that the observed charged species are the singly charged ones.

DOI: 10.1103/PhysRevB.79.155411 PACS number(s): 61.48.−c, 36.40.Qv, 71.15.Nc

I. INTRODUCTION

Heterofullerenes are synthesized by doping pristine fullerene cages such as the prototypical C_{60}. In these systems, the main result of doping is a rearrangement of the electronic distribution on specific locations of the cage, the new bonding nature of the affected sites depending on the impurities identity and amount.[1–7] By focusing on substitutional doping, in which foreign atoms replace carbon atoms, the case of silicon doping stands out as the most studied one.[8–19] Most likely, this is due to the intriguing behavior of the Si atoms prone to sp^3 bonding but constrained to arrange in a sp^2 fashion within the fullerene geometry.[13]

In this context, the last decade has witnessed intense experimental and theoretical efforts devoted to the assessment of the upper limit of Si-C replacements compatible with enduring stability of fullerenelike networks.[20–24] According to a combination of mass spectroscopy and photofragmentation measurements, this limit could be set to 12.[20,21] This estimate did not rule out the occurrence of a larger number of Si-C replacements, their detection being simply hampered by the experimental uncertainties due to the limited mass-spectra resolution. Theory has played a major role to elucidate this issue, throughout a series of density-functional theory (DFT) calculations addressing both structural and electronic properties of $C_{60-n}Si_n$ clusters.[13,14,22–26] By beginning with the case of one and two doping Si atoms, calculations have been extended first up to 12 (Refs. 22, 23, 25, 27, and 28) and then up to 30.[24,26] In all these systems, the binding energy is lowered when two neighboring and yet spatially segregated regions form, each one populated exclusively by silicon or carbon atoms. By using first-principles molecular dynamics (FPMD) and a local charge analysis, we were able to conclude that a transition from thermally stable to thermally unstable $C_{60-n}Si_n$ should occur at $n=20$. The value $n=20$ corresponds to an equal number of *outer* Si atoms (bonding neighboring C atoms at the Si-C region border) and *inner* Si atoms (not bound to any C atom).[24] The question arises on how these results can be also representative of the case of charged Si-doped heterofullerenes. This issue is motivated by the actual setup of mass spectroscopy and photofragmentation experiments,[8–10,20,21] in which the cluster species are produced in their charged states. Both positive and negative charge states are *a priori* observable. Very recently, we have provided preliminary indications on the effect of a positive or negative charge on the stability of $C_{30}Si_{30}$.[29,30] Based on optimized structures at $T=0$ K, we found that neither the structure nor the overall charge topology of $C_{30}Si_{30}^{-}$ and of $C_{30}Si_{30}^{+}$ differ significantly from the ones of neutral $C_{30}Si_{30}$. The purpose of this paper is to improve and complete upon this analysis, by considering in a combined way: (a) the case of doubly charged heterofullerenes, providing information on the existence of a charge stability threshold and (b) the dynamical behavior of all studied charged species, singly and doubly charged, both positively and negatively. This allows to achieve a comprehensive picture of charge effects in Si-doped heterofullerenes. To fulfill these goals, we rely on density-functional theory through geometry optimization, charge population analysis, and first-principles molecular dynamics. This paper is organized as follows. We first describe in Sec. II our methodology and the reasons underlying the choice of a specific isomer of $C_{30}Si_{30}$. In Sec. III we describe our results on the bond lengths, Mulliken charges and dynamical behavior of singly and doubly charged $C_{30}Si_{30}$ heterofullerenes. The paper ends with some conclusive remarks collected in Sec. IV.

II. METHODOLOGY AND CHOICE OF THE SYSTEMS

The calculations are performed within the framework of the FPMD approach.[31,32] Further technical details can be found in our previous publications devoted to the same

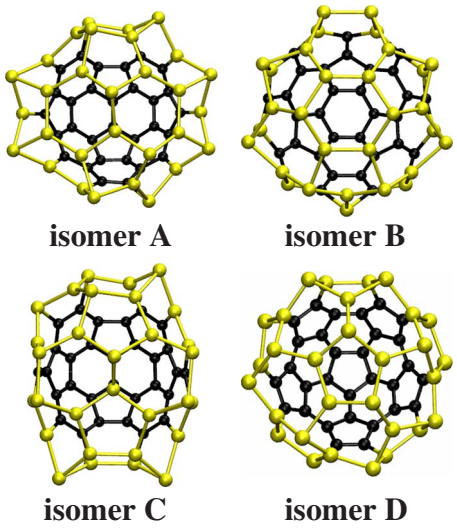

FIG. 1. (Color online) Four low lying energy different isomers of $C_{30}Si_{30}$. The isomer considered in this work is isomer D. Black spheres denote C atoms and yellow ones denote Si atoms. This figure is generated with VMD version 1.8.6 (Ref. 40).

topic,[24,26,27] where we have reported a large number of structurally stable Si-doped heterofullerenes. These have been produced by considering a previously optimized $C_{60-n+1}Si_{n-1}$ structure, imposing a new C-Si replacement and then optimizing the new structure $C_{60-n}Si_n$ (Ref. 33). Spin effects are accounted for within the spin density version of DFT, combined with a generalized gradient approximation.[34] It has to be reminded that the plane-wave scheme can be applied to an isolated cell within FPMD by using the Hockney method.[35] This approach is more time-consuming than periodic calculations, especially in the case of extensive molecular dynamics runs. However, in the particular case of doubly charged systems, it might provide a more realistic spatial distribution of charges, corresponding to distinct structural and dynamical properties. To clarify this issue, we obtained two sets of results (in the periodic and isolated frameworks, respectively) for the bond lengths, Mulliken charges, and the dynamical behavior at finite temperatures of the doubly charged systems. Fully relaxed structures are obtained by minimizing the forces on all atoms using direct inversion in the iterative subspace.[32] Optimization of the ionic positions is performed without constraint on the structure and is allowed to proceed until the largest force component is less than 5×10^{-4} a.u. and the average force is 1 order of magnitude smaller.

In this work we focus on the $C_{30}Si_{30}$ isomer (isomer D in Fig. 1) that was the object of an intensive first-principles molecular study on the neutral case.[24] By choosing this same configuration for the charged states also, we allow a suitable comparison to be carried out among the four different charged heterofullerenes and their neutral counterpart. We take this structure as the starting configuration for optimization of the charged systems. The total charge is changed by subtracting (for positively charged case) or adding (for negatively charged case) one or two electrons. This specific configuration lies only 0.53 eV above the lowest energy isomer of $C_{30}Si_{30}$ in the neutral case.[30] In Table I, the energy of this isomer is compared to those pertaining to three other isomers, A, B, and C (neutral and charged) of $C_{30}Si_{30}$ (Fig. 1). The calculations on the charged systems have been carried out by using both the periodic and the isolated cells. Isomers A, B, and C were found to lie systematically at lower energies than isomer D, isomer A being the most stable (see Table I). Addition or subtraction of one or two charges changes only moderately the energy ordering. In particular, one notices that isomer D is higher in energy by at least 0.5 eV than the lowest energy isomer for both the neutral and the charged states.

TABLE I. Energy ordering of the isomers A, B, C, and D (neutral and charged) of $C_{30}Si_{30}$. The energy differences (in eV) with respect to the lowest energy isomer are given in parentheses. The labels P and I stand for calculations carried out within the periodic and the isolated frameworks, respectively.

Isomer	Neutral	+1	+2	−1	−2
A(P)	1	1	1	1	1
B(P)	2 (0.05)	3 (0.11)	3 (0.14)	2 (0.08)	3 (0.23)
C(P)	3 (0.09)	2 (0.06)	2 (0.03)	3 (0.15)	2 (0.08)
D(P)	4 (0.53)	4 (0.53)	4 (0.54)	4 (0.51)	4 (0.55)
A(I)	1	1	1	1	1
B(I)	2 (0.07)	3 (0.13)	3 (0.15)	2 (0.08)	3 (0.32)
C(I)	3 (0.18)	2 (0.12)	2 (0.04)	3 (0.27)	2 (0.28)
D(I)	4 (0.60)	4 (0.57)	4 (0.61)	4 (0.61)	4 (0.74)

A large amount of computational resources have been devoted to the study of the thermal behavior of the charged species. Beginning from an initial temperature $T=1000$ K applied to the optimized configurations, temperatures are increased stepwise by 500 K every 4 ps up to 2000 K, then by 1000 K every 4 ps to monitor the occurrence of fragmentation. At each temperature, thermalization is controlled via the Nosé-Hoover thermostat.[36,37] To ensure Born-Oppenheimer adiabaticity, the same approach has been used for the fictitious electronic degrees of freedom at the highest temperatures and for all charged systems.[38]

III. RESULTS

A. Bond lengths

By referring to isomer D in the charged states, bond lengths obtained via structural optimization carried out on $C_{30}Si_{30}^{-}$, $C_{30}Si_{30}^{+}$, $C_{30}Si_{30}^{--}$, and $C_{30}Si_{30}^{++}$ are given in Table II and compared with the neutral case. Two sets of data are presented for $C_{30}Si_{30}^{--}$ and $C_{30}Si_{30}^{++}$, referring to the periodic and isolated frameworks, respectively. In the table, *ph* denotes the bond between a pentagon and a hexagon, while *hh* denotes the bond between two hexagons. It is useful to classify the Si atoms in terms of their belonging or not to the frontier with C (outer Si atoms, Si_{out} vs inner Si atoms Si_{in}). Inner atoms can be further labeled as first (Si_{fi} hereafter), second (Si_{se}), or third (Si_{th}) neighbors of outer Si atoms. A view of the charged systems is given in Fig. 2 to highlight the similarity among their shapes. As seen in Table II, C-C and Si-C bonds are not affected by the charge state. Also,

TABLE II. Bond lengths in neutral, singly charged, and doubly charged cases. For Si-Si bonds, bond lengths of inner and outer Si atoms are presented separately. Only the smallest and the largest values are given.

Charge state		Si-Si (Å) Outer	Si-Si (Å) Inner	Si-C (Å)	C-C (Å)
0 (neutral)	*ph*	2.30–2.41	2.35–2.48		1.45–1.49
	hh		2.31–2.40	1.85–1.91	1.40–1.44
+1 charged	*ph*	2.30–2.41	2.36–2.49		1.45–1.49
	hh		2.32–2.39	1.86–1.92	1.40–1.44
+2 charged	*ph*	2.30–2.41	2.36–2.48		1.44–1.50
(periodic)	*hh*		2.32–2.40	1.86–1.92	1.40–1.44
+2 charged	*ph*	2.31–2.39	2.35–2.47		1.44–1.49
(isolated)	*hh*		2.31–2.39	1.86–1.91	1.40–1.44
−1 charged	*ph*	2.30–2.40	2.35–2.51		1.45–1.49
	hh		2.33–2.43	1.85–1.91	1.40–1.45
−2 charged	*ph*	2.30–2.40	2.31–2.53		1.45–1.49
(periodic)	*hh*		2.32–2.45	1.85–1.91	1.40–1.45
−2 charged	*ph*	2.30–2.42	2.34–2.52		1.45–1.49
(isolated)	*hh*		2.34–2.43	1.86–1.92	1.40–1.45

adding one or two positive charges results in negligible variations in Si-Si distances. In the negative charge case, the most relevant changes in the Si-Si bonds occur for the double *hh* bonds, their upper values being increased by 2% with respect to the neutral case (2.45 Å against 2.40 Å). Bond stretching in *hh* bonds can be attributed to their double bond nature and stems from the additional repulsion between Si centers bearing charges of equal sign. This occurs to a lesser extent in *ph* bonds, especially for $C_{30}Si_{30}^{--}$ (upper limit 2.53 Å against 2.48 Å in the neutral case). Account of Table II reveals that the bond lengths obtained from the periodic and isolated calculations are very close, with differences not exceeding 1%.

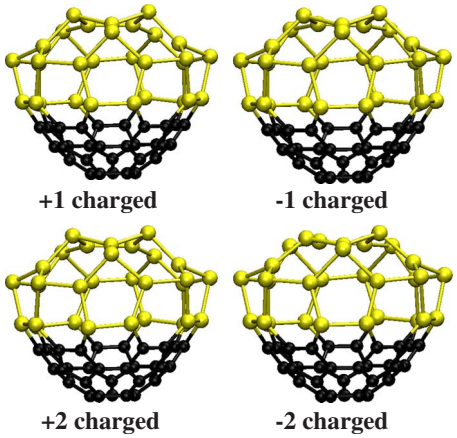

FIG. 2. (Color online) Three-dimensional representations of the charged isomers $C_{30}Si_{30}^{+}$, $C_{30}Si_{30}^{-}$, $C_{30}Si_{30}^{++}$, and $C_{30}Si_{30}^{--}$ obtained from the neutral isomer D. Black spheres denote C atoms and yellow ones denote Si atoms. This figure is generated with VMD version 1.8.6 (Ref. 40).

B. Mulliken charge analysis

We obtained the Mulliken charge topology for $C_{30}Si_{30}$, $C_{30}Si_{30}^{-}$, $C_{30}Si_{30}^{+}$, $C_{30}Si_{30}^{--}$, and $C_{30}Si_{30}^{++}$ (Fig. 3). Calculations referred to in Fig. 3 have been performed in the periodic cells. Common to the five systems is the existence of a C-Si border made of negatively charged C atoms and positively charged Si atoms. In the neutral and in the singly charged cases, the inner Si region features charge alternation, vanishing positive and negative values being observable. Nearest

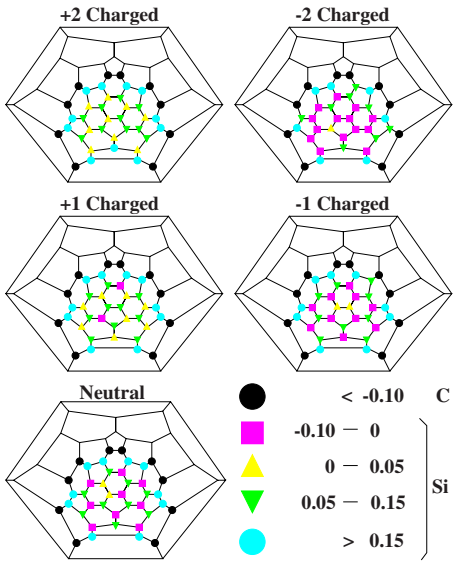

FIG. 3. (Color online) A flattened two-dimensional view of isomer D in the different charge states. The color codes correspond to the values of the Mulliken charges. Calculations on the charged systems have been carried out in the periodic cell configuration.

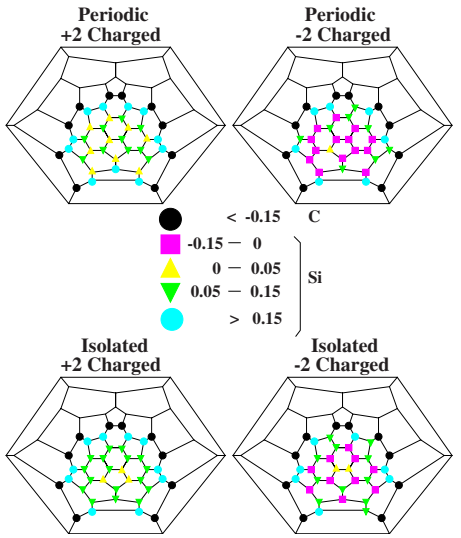

FIG. 4. (Color online) A flattened two-dimensional view of isomer D with the values of the Mulliken charges. A comparison is provided between the Mulliken charges obtained using the periodic and the isolated cell boundary conditions for the case of $C_{30}Si_{30}^{++}$ and $C_{30}Si_{30}^{--}$.

neighbors carrying opposite signs are largely predominant among Si_{fi}, Si_{se}, and Si_{th} atoms. The situation changes drastically in the case of $C_{30}Si_{30}^{--}$ and $C_{30}Si_{30}^{++}$. In $C_{30}Si_{30}^{++}$, the entire set of Si_{in} atoms is charged positively. Similarly, in $C_{30}Si_{30}^{--}$, most Si_{in} atoms bear negative charges, with fewer bonds between charges of opposite sign. In Fig. 4, the Mulliken charge topologies obtained for the periodic cells and the isolated cells options are compared. Positive charges remain largely predominant among Si_{in} atoms for $C_{30}Si_{30}^{++}$. In the $C_{30}Si_{30}^{--}$ case, the effect of removing the periodicity amounts to a fewer number of neighbors carrying charges of the same sign, leading to a charge topology similar to the one of $C_{30}Si_{30}^{-}$ case. This means that periodicity can induce an artificial clustering of charges of the same sign in the inner region, contributing to destabilize the doped fullerene network. For this reason, the isolated system option appears the best suited to achieve a realistic description of the charge distribution on the cage. A smaller number of nearest neighbors of the same charge sign appear in the isolated calculation for $C_{30}Si_{30}^{--}$ (Fig. 4, bottom part), while the charge distribution is much less affected in $C_{30}Si_{30}^{++}$. Interestingly, in $C_{30}Si_{30}^{--}$, the absolute values of the negative charges are higher than for the single negatively charged system, being comprised in between 0 and 0.15 for $C_{30}Si_{30}^{--}$ and in between 0 and 0.10 for $C_{30}Si_{30}^{-}$.

C. Dynamical behavior

The different charge topologies encountered as a function of the charged state are expected to have profound implications on the thermal behavior of these systems. As shown for the neutral case, the local environment of Si_{in} atoms[24] is highly sensitive to anharmonic effects. To highlight this point, we turn to the time fluctuations with respect to the initial atomic positions for the Si_{out} and the set of Si atoms

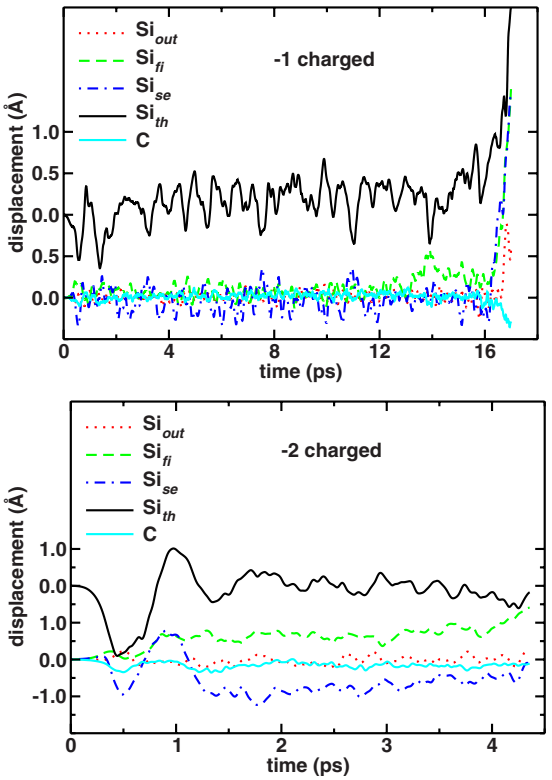

FIG. 5. (Color online) Temporal evolution of the coordinates of relevant C and Si atoms in $C_{30}Si_{30}^{-}$ (upper panel) and $C_{30}Si_{30}^{--}$, both obtained in the periodic cell framework. The values are calculated with respect to the $t=0$ positions and, in the case of the Si_{th} atoms, moved up on the y axis by 1 Å for $C_{30}Si_{30}^{-}$ and by 2 Å for $C_{30}Si_{30}^{--}$ for clarity. The displacements are calculated with respect to the center of mass of the system, positive and negative values meaning that the atoms are farther apart or closer to the initial position at $t=0$, respectively. This also applies to Figs. 6, 7, and 9.

Si_{in}, obtained via FPMD (Fig. 5). Nearest-neighbor carbon atoms are also included. Fragmentation in the neutral case was associated to an outward movement of the two Si_{th} atoms over the time interval 16–21 ps. Cage disruption was found at $T=3000$ K and driven by elongation of the Si_{in}-Si_{in}

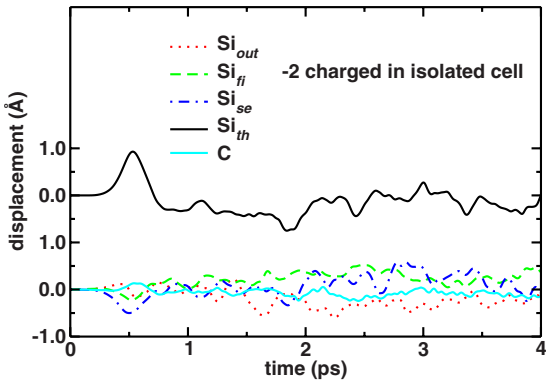

FIG. 6. (Color online) Temporal evolution of the coordinates of relevant C and Si atoms in $C_{30}Si_{30}^{--}$ (isolated cell calculations). The values are calculated with respect to the $t=0$ positions and, in the case of the Si_{th} atoms, moved up on the y axis by 2 Å for clarity.

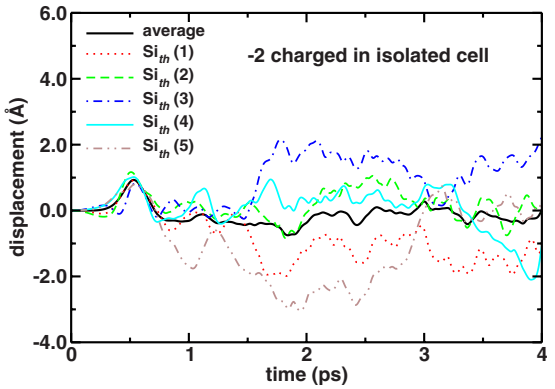

FIG. 7. (Color online) Temporal evolution of the coordinates of Si atoms third neighbors (Si_{th}) of Si atoms bonded to C atoms in $C_{30}Si_{30}^{--}$ (isolated cell calculations). The values are calculated with respect to the $t=0$ positions.

distances.[24] A close situation is encountered for $C_{30}Si_{30}^{-}$, with enhanced variations for Si_{th} atoms and fragmentation occurring after a time interval (12 ps), equally at $T=3000$ K (Fig. 5). The predominant amount of nearest neighbors of equal sign among Si_{in} atoms (in the periodic cell case) or the intensity of the repulsion between charges of equal sign (in the isolated cell case) induce a different behavior in $C_{30}Si_{30}^{--}$. This is shown in Fig. 5 for the periodic cell case and in Fig. 6 for the isolated cell case, where for each subset of Si_{in} atoms (Si_{fi}, Si_{se}, Si_{th}) and for the Si_{out} atoms the average values taken on all atoms of the set are reported. In Fig. 7 we focus on the behavior of the Si_{th} atoms for the isolated cell case. An enhanced mobility of each individual atom is clearly detectable. As a consequence, the innermost shell of Si atoms departs very rapidly from the initial positions, triggering an abrupt loss of stability, visualized in Fig. 8. Enhanced displacements are found not only for the innermost Si_{th}, but also for Si_{se} and Si_{fi} (see Figs. 5 and 6), as a result of

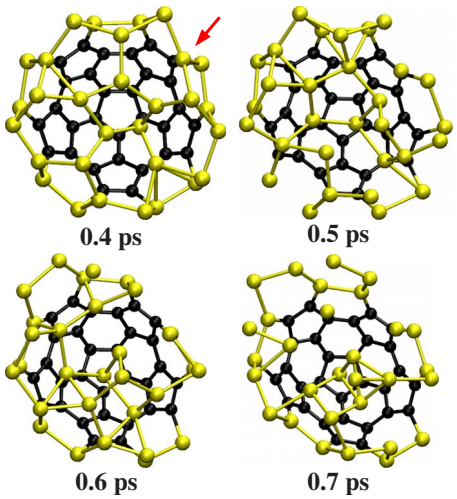

FIG. 8. (Color online) Snapshots of the dynamical evolution at $T=1000$ K of $C_{30}Si_{30}^{--}$ (periodic cell calculations) in the interval 0.4–0.7 ps. The arrow shows the *hh* bond first to break among the Si-Si connections. This figure is generated with VMD version 1.8.6 (Ref. 40).

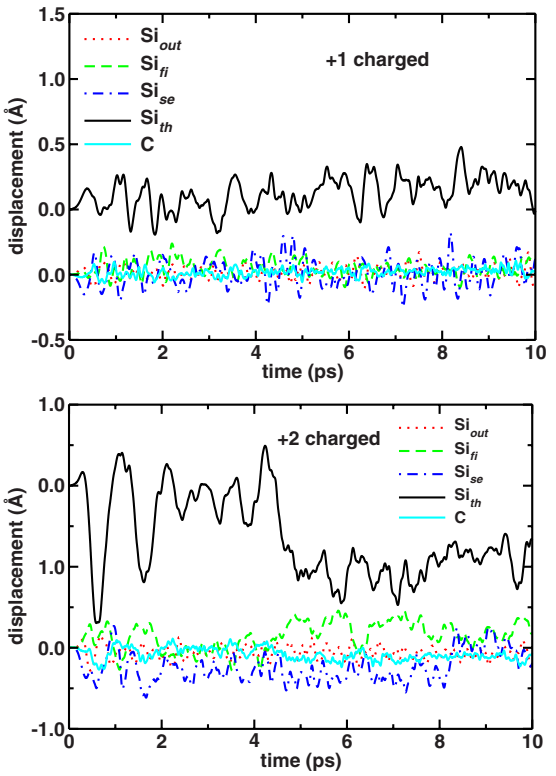

FIG. 9. (Color online) Temporal evolution of the coordinates of relevant C and Si atoms in $C_{30}Si_{30}^{+}$ (upper panel) and $C_{30}Si_{30}^{++}$, both obtained in the periodic cell framework. The values are calculated with respect to the $t=0$ positions and, in the case of the Si_{th} atoms, moved up on the y axis by 1 Å for $C_{30}Si_{30}^{+}$ and by 2 Å for $C_{30}Si_{30}^{++}$ for clarity.

a global rearrangement of the Si part of the cage. Indeed, in Fig. 8, the heterofullerene is found to open up at the location of an hexagon via elongation of a *hh* bond involving one Si_{fi} atom and one Si_{se} atom. This induces a sudden change in the nature of bonding for most Si atoms, increasing the number of sp^3 configurations at the expense of the initial sp^2 ones.

The above picture is confirmed by the consideration of the positively charged species (periodic cell calculations). In Fig. 9 we compare the behavior of $C_{30}Si_{30}^{+}$ and $C_{30}Si_{30}^{++}$ on a time scale of 10 ps. While in both cases the Si_{th} have a marked tendency to depart from their initial positions, the observed changes are larger in $C_{30}Si_{30}^{++}$, inducing fragmentation on a shorter time interval.

IV. CONCLUSIONS

We have shown that the stability of Si-doped heterofullerenes is highly reduced in the doubly charged case, giving a clear indication on the existence of a charge threshold for the observation of these systems. This conclusion is consistent with the experimental evidence, based on a large share of results obtained on singly charged species.[8–11,20,21] We found that the thermal stability of singly charged species is not significantly different from the one of their corresponding neutral counterpart. Addition or removal of a further electron drives rapid cage disruption upon inclusion of

thermal motion. In addition, we were able to show that our conclusions hold true both in the periodic and in the isolated cell option for the boundary conditions, in spite of a different distribution of charges on the silicon atoms. In view of these pieces of evidence, the present study allows to apply the results on the thermal stability collected for the neutral case to the case of single charged Si-doped heterofullerenes, by ruling out doubly charged species as potentially observable Si-doped heterofullerenes. Work is in progress to apply this methodology to the case of supported Si-doped fullerenes, along the lines pioneered in previous work devoted to cluster deposition.[39]

[1] I. M. L. Billas, W. Branz, N. Malinowski, F. Tast, M. Heinebrodt, T. P. Martin, C. Massobrio, M. Boero, and M. Parrinello, Nanostruct. Mater. **12**, 1071 (1999).

[2] Q. Kong, Y. Shen, L. Zhao, J. Zhuang, S. Qian, Y. Li, Y. Lin, and R. Cai, J. Chem. Phys. **116**, 128 (2002).

[3] H. Jiao, Z. Chen, A. Hirsch, and W. Thiel, J. Mol. Model. **9**, 34 (2003).

[4] J. Pattanayak, T. Kar, and S. Scheiner, J. Phys. Chem. A **107**, 4056 (2003).

[5] T. M. Simeon, I. Yanov, and J. Leszczynski, Int. J. Quantum Chem. **105**, 429 (2005).

[6] Z. Chen and R. B. King, Chem. Rev. **105**, 3613 (2005).

[7] O. Vostrowsky and A. Hirsch, Chem. Rev. **106**, 5191 (2006).

[8] T. Kimura, T. Sugai, and H. Shinohara, Chem. Phys. Lett. **256**, 269 (1996).

[9] J. L. Fye and M. F. Jarrold, J. Phys. Chem. A **101**, 1836 (1997).

[10] M. Pellarin, C. Ray, P. Mélinon, J. Lermé, J. L. Vialle, P. Kéghélian, A. Perez, and M. Broyer, Chem. Phys. Lett. **277**, 96 (1997).

[11] C. Ray, M. Pellarin, J. L. Lermé, J. L. Vialle, M. Broyer, X. Blase, P. Mélinon, P. Kéghélian, and A. Perez, Phys. Rev. Lett. **80**, 5365 (1998).

[12] I. M. L. Billas, F. Tast, W. Branz, N. Malinowski, M. Heinebrodt, T. P. Martin, M. Boero, and C. Massobrio, Eur. Phys. J. D **9**, 337 (1999).

[13] I. M. L. Billas, C. Massobrio, M. Boero, M. Parrinello, W. Branz, F. Tast, N. Malinowski, M. Heinebrodt, and T. P. Martin, J. Chem. Phys. **111**, 6787 (1999).

[14] W.-D. Cheng, D.-S. Wu, H. Zhang, D.-G. Chen, and H.-X. Wang, Phys. Rev. B **66**, 085422 (2002).

[15] C.-C. Fu, J. Fava, R. Weht, and M. Weissmann, Phys. Rev. B **66**, 045405 (2002).

[16] I. Zanella, A. Fazzio, and A. J. R. da Silva, J. Phys. Chem. B **110**, 10849 (2006).

[17] P. A. Marcos, J. A. Alonso, and M. J. López, J. Chem. Phys. **126**, 044705 (2007).

[18] P. Mélinon, B. Masenelli, F. Tournus, and A. Perez, Nature Mater. **6**, 479 (2007).

[19] L. Koponen, M. J. Puska, and R. M. Nieminen, J. Chem. Phys. **128**, 154307 (2008).

[20] M. Pellarin, C. Ray, J. Lermé, J. L. Vialle, M. Broyer, X. Blase, P. Kéghélian, P. Mélinon, and A. Perez, Eur. Phys. J. D **9**, 49 (1999).

[21] M. Pellarin, C. Ray, J. Lermé, J. L. Vialle, M. Broyer, X. Blase, P. Kéghélian, P. Mélinon, and A. Perez, J. Chem. Phys. **110**, 6927 (1999).

[22] C.-C. Fu, M. Weissmann, M. Machado, and P. Ordejón, Phys. Rev. B **63**, 085411 (2001).

[23] M. Menon, J. Chem. Phys. **114**, 7731 (2001).

[24] M. Matsubara, J. Kortus, J. C. Parlebas, and C. Massobrio, Phys. Rev. Lett. **96**, 155502 (2006).

[25] P. A. Marcos, J. A. Alonso, L. M. Molina, A. Rubio, and M. J. López, J. Chem. Phys. **119**, 1127 (2003).

[26] M. Matsubara and C. Massobrio, J. Phys. Chem. A **109**, 4415 (2005).

[27] M. Matsubara and C. Massobrio, J. Chem. Phys. **122**, 084304 (2005).

[28] P. A. Marcos, J. A. Alonso, and M. J. López, J. Chem. Phys. **123**, 204323 (2005).

[29] M. Matsubara and C. Massobrio, Appl. Phys. A **A86**, 289 (2007).

[30] M. Matsubara and C. Massobrio, Solid State Phenom. **129**, 95 (2007).

[31] R. Car and M. Parrinello, Phys. Rev. Lett. **55**, 2471 (1985).

[32] We have used the code CPMD: CPMD Version 3.11.1, Copyright IBM Corp (1990–2006), MPI für Festkörperforschung Stuttgart (1997–2001).

[33] Coordinates of published structures for Si-doped heterofullerenes are available upon request from the authors.

[34] A. D. Becke, Phys. Rev. A **38**, 3098 (1988).

[35] R. W. Hockney, Methods Comput. Phys. **9**, 136 (1970).

[36] S. Nosé, Mol. Phys. **52**, 255 (1984).

[37] W. G. Hoover, Phys. Rev. A **31**, 1695 (1985).

[38] P. E. Blöchl and M. Parrinello, Phys. Rev. B **45**, 9413 (1992).

[39] G. Vandoni, C. Félix, and C. Massobrio, Phys. Rev. B **54**, 1553 (1996).

[40] W. Humphrey, A. Dalke, and K. Schulten, J. Mol. Graph. **14**, 33 (1996).